PERFORMANCE ANALYSIS OF PARALLEL FLOW SINGLE AND DOUBLE EFFECT ABSORPTION CYCLES

Mohammad Seraj [1] , M. Altamush Siddiqui [2]

Assistant Professor, Department of Mechanical Engineering, Mangalayatan University, Aligarh, India[1]

Professor, Department of Mechanical Engineering, Aligarh Muslim University, Aligarh, India[2]

Abstract: Thermodynamic analysis of parallel flow single and double effect LiBr-H_2O absorption system has been carried out. In the single effect cycle, the refrigerant leaving the evaporator is divided to flow in parallel and get absorbed partly in a heat recovery absorber and the remaining in a heat rejecting absorber. This reduces heat load of the generator to a great extent and hence, improves COP of the cycle. Similarly in the double effect parallel flow cycle, the solution leaving the absorber is divided into two parts, one being sent to the main generator and the other to the secondary generator. Such type of arrangement in the double effect system increases COP of the cycle as compared to the series flow cycle. The refrigerant distribution ratio (RDR) in the single effect refrigerant-parallel flow cycle and the solution distribution ratio (SDR) in the double effect solution-parallel flow cycle have been optimized. The optimization results, corresponding to the maximum COP, yield: RDR=0.30 and SDR=0.45. A comparative study between the single effect simple cycle, single effect cycle using heat recovery absorber, double effect parallel flow cycle and double effect series flow cycle has been presented. The analysis has been done by varying evaporator temperature (T_e) from 5^oC to 12.5^oC and condenser/absorber temperature (T_c) from 30^oC to 40^oC.

Keywords: Parallel Flow, Double Effect, LiBr-H_2O, Absorption Cycles

I. INTRODUCTION

The absorption refrigeration system utilizes non CFC's natural refrigerant and is therefore, more environment-friendly. Also, it consumes less electricity and uses waste heat/low grade energy for its operation. Most of the absorption cooling system use either LiBr-H_2O or NH_3-H_2O solutions. The LiBr-H_2O system can operate at a low generator temperature with better coefficient of performance than NH_3-H_2O system. However, COP of absorption system is relatively less as compared to the compression system. Therefore, research is in progress and several modifications have been made in the cycle to improve its performance.

Asdrubali and Grignaffini [1] experimentally verified the performance of single-stage LiBr-H_2O absorption machine. Optimization of the generator temperature in H_2O-NH_3, $LiNO_3$-NH_3, $NaSCN$-NH_3 and LiBr-H_2O absorption cycles have been carried out by Siddiqui [2] for minimum cost of the energy sources: (biogas, LPG and solar collector). Gommed and Grossman [3] investigated the performance of single effect cycle and various configuration of double-effect absorption refrigeration cycle using LiBr-H_2O pair, under varying operating conditions. Lee and Sheriff [4] presented the second law analysis of various double effect LiBr-H_2O absorption chillers for a chilled water temperature of 7.22°C and cooling water temperatures at 29.4 and 35°C. Khaliq and Kumar [5] examined a double-effect vapour absorption refrigeration system. Arun et al. [6] compared the performance of double-effect LiBr-H_2O absorption system and found that the maximum attainable COP for parallel flow cycle is greater than for the series flow cycle.

Oh et al. [7] have carried analysis on air-cooled LiBr-H_2O absorption heat pump of parallel flow double effect system. They have suggested the possible optimum range of Solution Distribution Ratio (SDR) as 0.35-0.4 for Δx=4% (Δx= difference of LiBr salt concentration in the solution entering and leaving the absorber). Xu and Dai [8] have conducted analysis and optimization of double effect parallel flow type absorption chiller and suggested that the system operation is safe when the SDR is close to 0.5. Wang et al. [9] have presented analysis of gas-fired air-cooled parallel flow double effect LiBr-H_2O system. They have simulated the system for some specific parameters and suggested the value of SDR=0.418.

Kaushik and Kumar [10] and Kandlikar[11] have carried thermodynamic study on an absorber heat recovery cycle. Saghiruddin and Siddiqui [12,13] performed economic analyses of some sources of energy for operating single effect absorption cycles with and without heat recovery absorber. Use of a heat recovery absorber improves the system performance and reduces the energy cost. In the analysis carried out by Saghiruddin and Siddiqui [12,13], the Refrigerant Distribution Ratio (RDR) in the heat recovery absorber has been simply considered as 0.5; although the COP varies with change in the value of the RDR.

II. SINGLE EFFECT ABSORPTION CYCLE

Figure 1 shows line diagram of the single effect absorption cycle, employing a heat recovery absorber and Fig. 2 represents the refrigeration process of the same cycle on PTX diagram. The absorber assembly has a heat recovery absorber (HRA) and a main absorber (A). The refrigerant coming from evaporator is distributed to flow parallel into two parts; one entering the heat recovery absorber (HRA) and the other to the main absorber. The refrigerant entering the HRA gets absorbed in the strong solution coming from the generator. This mixture in the HRA then goes to the main absorber and absorbs the remaining part of the refrigerant coming from the evaporator. Thus, a weak solution is formed in the main absorber which is sent via the heat recovery absorber (HRA) to take the heat evolved during absorption in the HRA. Thus, a heated solution is obtained at exit of absorber which reduces the requirement of heat input in the generator. This solution, before reaching the generator is passed through a preheater to further heat it by means of hot solution coming from the generator. Since use of HRA decreases heat input to the generator in addition to the preheater therefore, the COP of system increases. The weak solution entering the generator via the preheater, releases refrigerant vapours after getting heat from the external source. The refrigerant produced in the generator is send o the condenser where it gets condensed after rejecting heat to the surrounding. The liquid refrigerant is then sent to the evaporator through a throttle valve, where it takes heat from the surrounding to be cooled and gets evaporated which is then sent to the absorber assembly to complete the cycle.
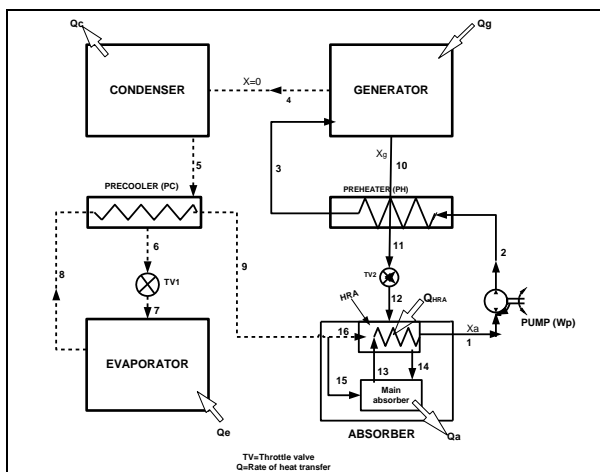

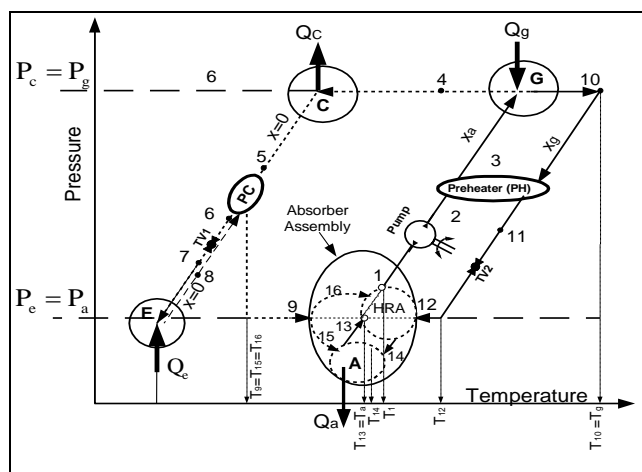Fig.1 Single Effect Refrigerant Parallel Flow Cycle with HRA   Fig. 2 Process of the cycle with HRA on P-T-X diagram

For thermodynamic analysis of the absorption system, the following equations have been obtained by making mass, concentration and energy balance on each component in Fig.1 as a control volume:

$$m_1 = m_4 x_g/(x_g - x_a) \tag{1}$$
$$m_{12} = m_{10} = m_4 x_a/(x_g - x_a) \tag{2}$$
$$m_{14} = m_{15} x_a/(x_{14} - x_a) \tag{3}$$
$$x_{14} = m_1 x_a/(m_1 - m_{15}) \tag{4}$$
$$Q_c = m_4 (h_4 - h_5) \tag{5}$$
$$Q_e = m_4 (h_8 - h_6) \tag{6}$$
$$Q_g = m_4 h_4 + m_{10} h_{10} - m_3 h_3 \tag{7}$$
$$Q_{HRA} = m_1 (h_1 - h_{13}) = m_{12} h_{12} + m_{16} h_{16} - m_{14} h_{14} \tag{8}$$
$$Q_a = m_{12} h_{12} + m_9 h_9 - m_1 h_{13} - Q_{HRA} \tag{9}$$

For the absorption system without heat recovery absorber, the heat $Q_{HRA}=0.0$, and state 13 will become state 1 making $h_{13} = h_1$; the system then becomes a single effect simple cycle. If $R_1 = RDR$ is the fraction of the evaporator-refrigerant allowed to pass into the heat recovery absorber (HRA) at state point 16 in the Fig.1, then $m_{16} = R_1 m_4$ and $m_{15} = (1-R_1)m_4$. In this analysis, effectiveness of the precooler and preheater are taken as: 0.75 and the absorber temperature is assumed to be equal to the condenser temperature.

III. DOUBLE EFFECT ABSORPTION CYCLE

Figure 3 shows the schematic diagram of a double effect parallel flow LiBr-H_2O absorption refrigeration cycle, the whole process of which has been shown on the P-T-X diagram in Fig. 4. It consists of two generators: a main generator (G) and a secondary generator (G_s), two condensers: a main condenser (C) and a secondary condenser (C_s), one

evaporator and one absorber. The main generator (G) and the secondary condenser (C_s) operate at high pressure ($P_3 = P_g$) while the secondary generator (G_s) and the main condenser (C) operate at medium pressure ($P_2 = P_c$). The evaporator and the absorber work at low pressure ($P_1 = P_e = P_a$). In this system, the weak solution, coming from absorber and leaving the low temperature heat exchanger is divided at state point 2D into two parts which then flow in parallel. One part of this solution goes to the main generator (G) through a high temperature heat exchanger (HX), and the other part goes to the secondary generator (G_s). The solution in main generator is heated at relatively high temperature to separate the refrigerant vapour from the solution. The vapour produced in the main generator (G,) enter the secondary condenser (C_s) and condenses into liquid. The heat of condensation at the secondary condenser is utilized by the secondary generator (G_s) to separate the refrigerant from the solution in the secondary generator.

The refrigerant produced in the main and secondary generators enter the main condenser at state points 7 and 16 where heat of condensation is rejected to the surrounding/sink. The liquid refrigerant from main condenser (C) then goes to the evaporator through a precooler and throttle valve where it vaporizes after extracting heat from the space to be cooled. The vapour leaving the evaporator then goes to the absorber where it gets absorbed by the strong solution coming from the two generators through the preheaters. This strong solution, coming from main and secondary generators, mix at a state point 17D before entering the absorber through the low temperature heat exchanger. The heat of absorption in the absorber is rejected to the surrounding/sink. The resulting weak solution in the absorber is again pumped to main and secondary generators. This completes the cycle of process in the system.
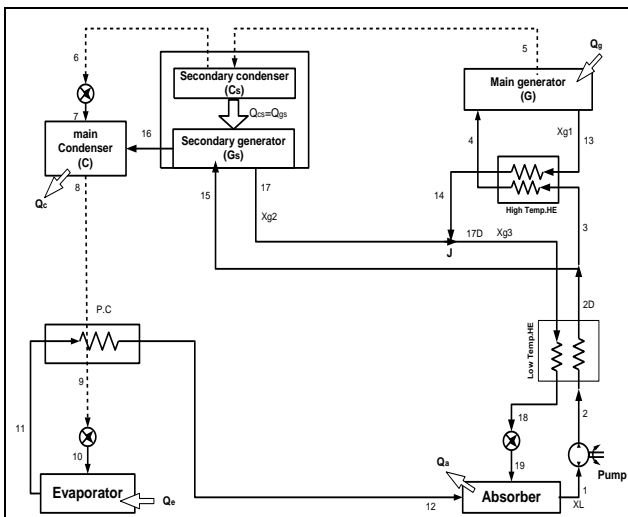

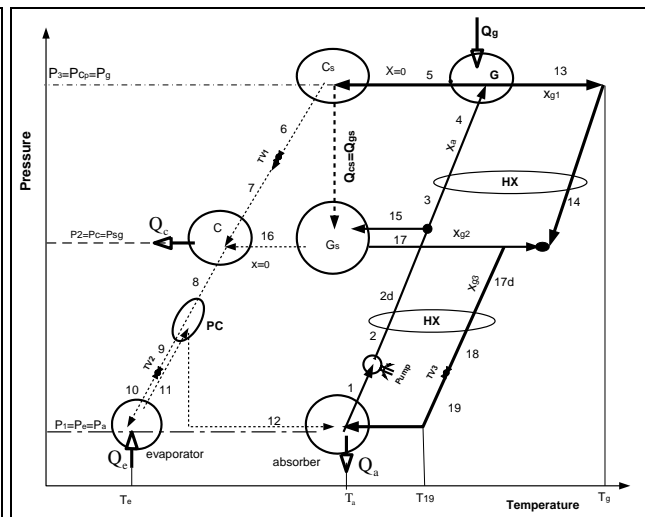Fig. 3 Double Effect Parallel Flow Cycle

Fig. 4 DE Parallel Flow Process on P-T-X diagram

The mass, concentration and energy balance on each component in the double effect parallel flow cycle (Fig. 3) as control volume, lead to the following equations:

$m_4 = m_5 + m_{13}$ (10)

$m_8 = m_7 + m_{16}$; $m_5 = m_6 = m_7$ (11)

$m_{17d} = m_{17} + m_{14}$; $m_{18} = m_{19} = m_{17d}$ (12)

$m_4 x_4 = m_5 x_5 + m_{13} x_{13}$ (13)

$m_{13} = m_4 x_4 / x_{g1}$;   since, $x_5 = 0$, $x_{g1} = x_{13}$ (14)

$m_{15} = m_{16} + m_{17}$ (15)

$m_{15} x_{15} = m_{17} x_{17}$ (16)

$m_{17} = m_{15} x_a / x_{g2}$; since $x_{15} = x_a$, $x_{16} = 0$, $x_{17} = x_{g2}$ (17)

At junction (J) where two strong solutions returning from main and secondary generator mix:

$m_{17d} = m_{14} + m_{17}$ (18)

Since, $x_{17d} = x_{g3}$, $m_{14} = m_{13}$, $x_{13} = x_{g1}$ and $x_{17} = x_{g2}$

$m_{17d} x_{g3} = m_{14} x_{g1} + m_{17} x_{g2}$ (19)

$m_{17d} h_{17d} = m_{14} h_{14} + m_{17} h_{17}$ (20)

Let solution distribution ratio (SDR) = $S_1 = m_3 / m_1$, then, $m_3 = m_4 = S_1 m_1$ and $m_{15} = (1 - S_1) m_1$ (21)

Now writing m_{13} and m_{17} in terms of S_1, equation (21) gives expression for x_{g3} as:

$$x_{g3} = \frac{1}{\left[\frac{S1}{X_{g1}} + \frac{(1-S1)}{X_{g2}}\right]}$$ (22)

Thus, one can get, $m_1 = m_8 x_{g3} / (x_{g3} - x_a)$ (23)

Heat transfer rates at various components are given by,

$Q_a = m_{19} h_{19} + m_{12} h_{12} - m_1 h_1$ (24)

$Q_c = m_7h_7 + m_{16}h_{16} - m_8h_8$ (25)

$Q_e = m_{10}(h_{11} - h_{10}); m_{10} = m_8$ and $Q_e = 12600$ kJ/h (26)

$Q_g = m_{13}h_{13} + m_5h_5 - m_4h_4$ (27)

$Q_{gs} = m_{17}h_{17} + m_6h_6 + m_{16}h_{16}$ (28)

$Q_{cs} = m_5h_5 + m_{15}h_{15}$ (29)

Heat balance at the secondary generator and condenser, requires : $Q_{gs} = Q_{cs}$

$COP = \dfrac{Q_e}{Q_g}$; (With neglecting pump work i.e. $W_p \approx 0$) (30)

$COP_{ideal} = \left(\dfrac{T_e}{T_c - T_e}\right) * \left(\dfrac{T_g - T_a}{T_g}\right)$ (31)

   In order to know the crystallization limit at critical locations in the system, following equation [14] has been used:

$X_c = 9.8459E\text{-}02(T-273.15) + 59.7995$; for $300 \leq T \geq 375$ (32)

Equations (30) to (32) are applicable to the all three cycles under study.

IV. RESULTS AND DISCUSSION

The thermodynamic and thermo-physical properties such as specific enthalpy, specific heat, saturation temperature/pressure and density of the working fluids in the absorption system, that is, pure refrigerant-water and the LiBr-H_2O mixture at different concentrations, have been evaluated using the equations taken from Refs. [14,15]. The analysis has been done for 1 TR (3.5kW) cooling capacity of the absorption system.

Figures 5 show variation in Coefficient of Performance of the single effect cycle using a heat recovery absorber (HRA) with generator temperature (T_g) for different values of the Refrigerant Distribution Ratio (RDR) and a set of temperatures: $T_e = 5^oC$ and $T_a = T_c = 35^oC$. It is seen that the COP, at first increases with T_g and then becomes almost constant. The COP also increases with increase in the values of RDR. This is because, higher flow rate of the refrigerant mass in the HRA results in higher rate of heat released ($=Q_{HRA}$), that raises energy level of the solution leaving the absorber, which in turn reduces heat input to the generator, leading to enhancement in COP of the system.
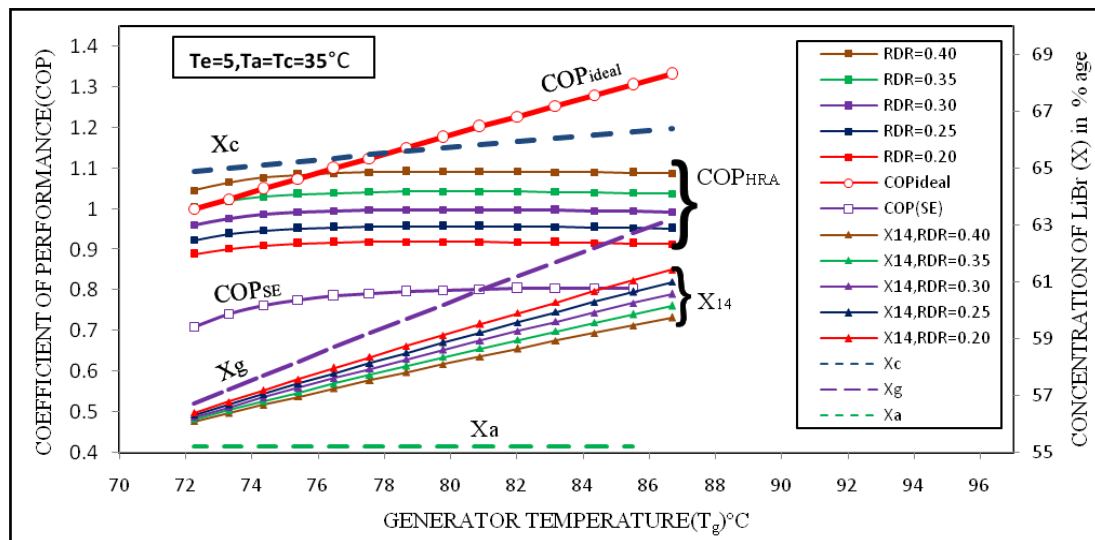

Fig. 5 Coefficient of performance of single effect cycle and LiBr solution concentration against the generator temperature at $T_e = 5$ °C, $T_a = T_c = 35$ °C.

The increase in COP with RDR, is however limited and should be below the ideal COP. The ideal COP increases almost linearly with T_g, as shown in the Fig.5. It is seen that actual COP of the system, remains below that of the COP_{ideal} only upto RDR=0.3. Thus, operation of the single effect cycle using HRA, is safe only when RDR≤0.3. However, it will give maximum COP when RDR=0.3.

The same trend is observed for other values of T_e and $T_a = T_c$. Therefore, RDR=0.3 is taken to be the optimum value for all values of T_e and $T_a = T_c$. COP of the simple-single stage cycle have also been shown. A drastic enhancement in COP of the system with the use of a Heat Recovery Absorber is observed. Also, the concentration of LiBr salt in the absorber (x_a), the generator (x_g) and the Heat Recovery Absorber (x_{14}) are shown in the Fig.5 along with the crystallization value (x_c) at state point 12, where there is possibility of crystallization of the solution having concentration x_g due to low temperature. The concentration of the solution leaving the HRA, that is x_{14}, increases linearly with T_g and is high for low values of RDR. This is because, the strong solution at concentration (x_g) will get less diluted after mixing with low mass of the refrigerant in the HRA and hence possesses high concentration at state

14. With increase in the refrigerant content, the concentration of the LiBr salt at state 14 will however, approach that in the absorber (x_a). Thus, variation in x_{14} will depend upon x_a, x_g and RDR.

In the double effect solution parallel flow cycle, since the weak solution leaving the absorber is distributed in two parts to flow in parallel, one going to the main generator and the other to the secondary generator, it is important to determine the optimum value of this solution distribution ratio (SDR). For this, COP of the double effect cycle with parallel solution distribution are obtained for different values of SDR (from 0.3 to 0.6) at fixed temperatures of T_e =5, 7.5, 10 & 12.5 ^{o}C and T_a=T_c =30, 35 & 40 ^{o}C. A typical plot in Fig. 6 shows that for all values of SDR, with increase in T_g the COP at first increases drastically and then becomes almost constant. Similar trend is observed for different sets of T_e and T_a=T_c. The highest value of COP for each value of SDR and the given sets of T_e and T_a=T_c are then identified. Here, the highest value of COP is either when it becomes constant or the system approaches the point of crystallization. The possibility of crystallization is that of the solution at concentration (x_{g1}) at state 14(x_{g1}> x_{g2}); which may the lowest temperature point with highest concentration.
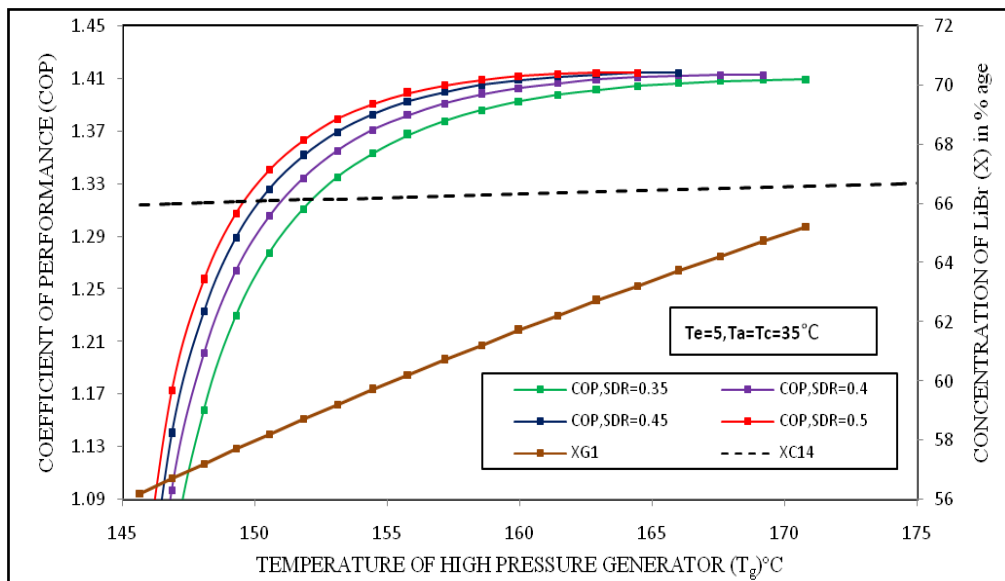

Fig. 6 Variation of COP and solution concentration with solution distribution ratio (SDR) in the double effect solution parallel flow cycle.

The highest value of COP, so obtained are then re-plotted against the solution distribution ratio SDR for all the sets of T_e and T_a=T_c, under study as shown in Figs. 7. Interestingly, one can see in Fig.6 that the COP increases with increase in SDR, reaches to maxima and then again decreases. Similar trend is observed for all sets of T_e and T_a=T_c. Thus, the optimum value of SDR corresponding to the maximum value of COP is selected. The optimum SDR for all sets of the variables under study thus, comes out to be 0.45.
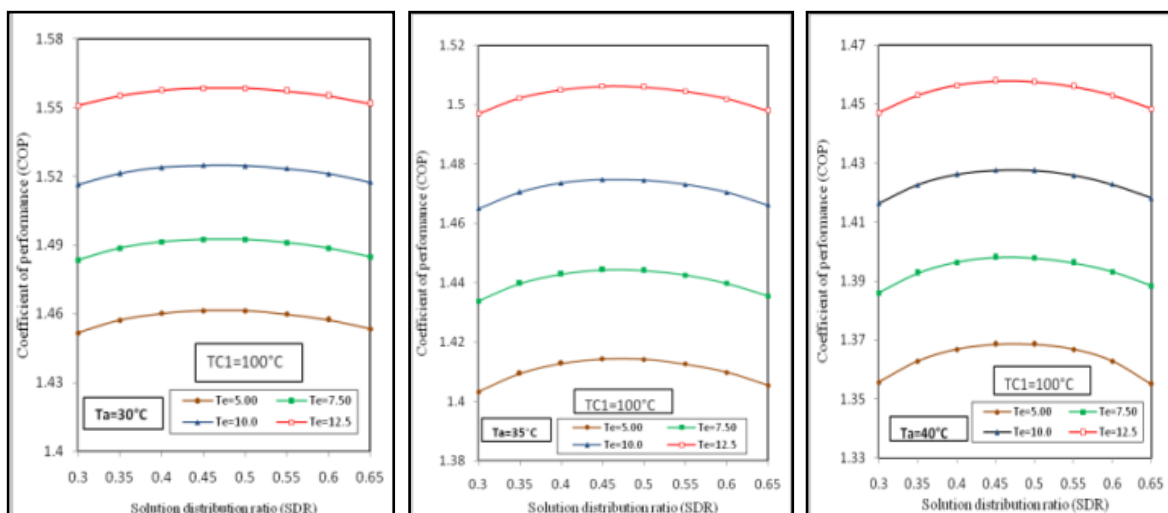

Fig. 7 Variation of COP of the double effect solution parallel flow cycle with the solution distribution ratio for different temperature in the evaporator and the condenser/absorber.

The coefficient of performance of the four cycles under study are plotted (for the optimum values of RDR=0.3 and SDR=0.45 in the parallel flows) against the generator temperature for different values of T_e at $T_a=T_c=30°C$ in Fig.8. It is seen that the COP for all conditions increase with the generator temperature, reach to maximum value and then become almost constant. One can again see drastic enhancement in the COP with the use of HRA in the single effect cycle. However, their generator temperatures do not change significantly. The double effect cycles, though operating at high generator temperature, result in very high values of COP; the double effect-solution-parallel flow cycle performing better than all.

Although, performance of the absorption system depends mainly on the generator heat load, the heat to be rejected from the absorber is equally important. It is, therefore, necessary to also see effect of the fluid distribution on the absorber cooling load. Fig.9 shows the absorber heat load in case of all the four cycles. In the single effect cycle using HRA, the absorber load becomes much lower than it could be in the cycle without HRA. Reduction of the absorber load by using HRA is because around 30% of the heat is extracted as Q_{HRA} which is also the representative of the refrigerant distribution ratio RDR=0.3.
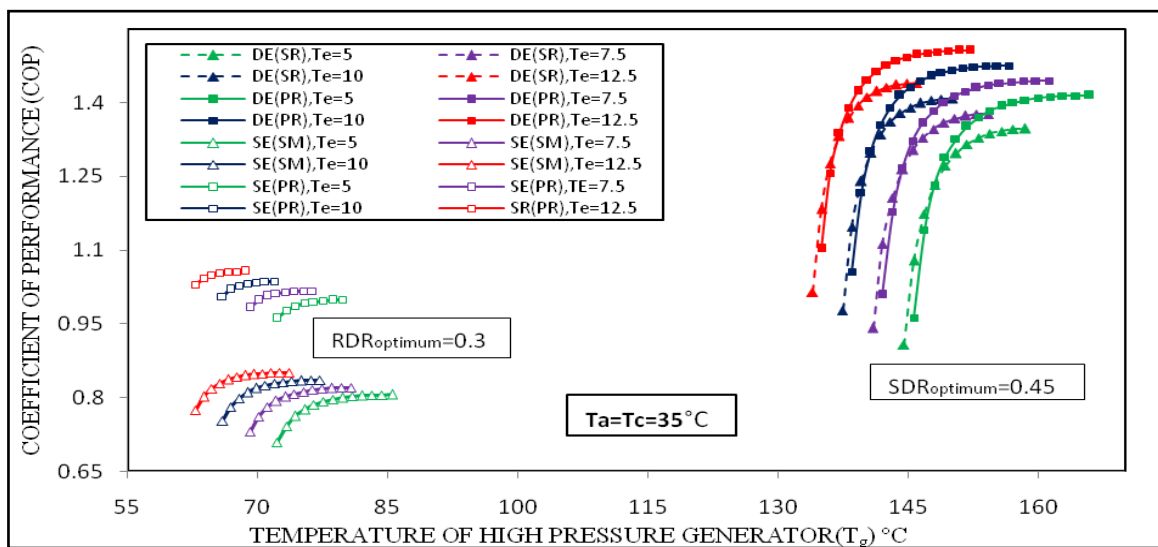

Fig.8 Variation of COP with the generator temperature for the single effect cycles (simple and with HRA) and the double effect cycles (parallel and series flows).
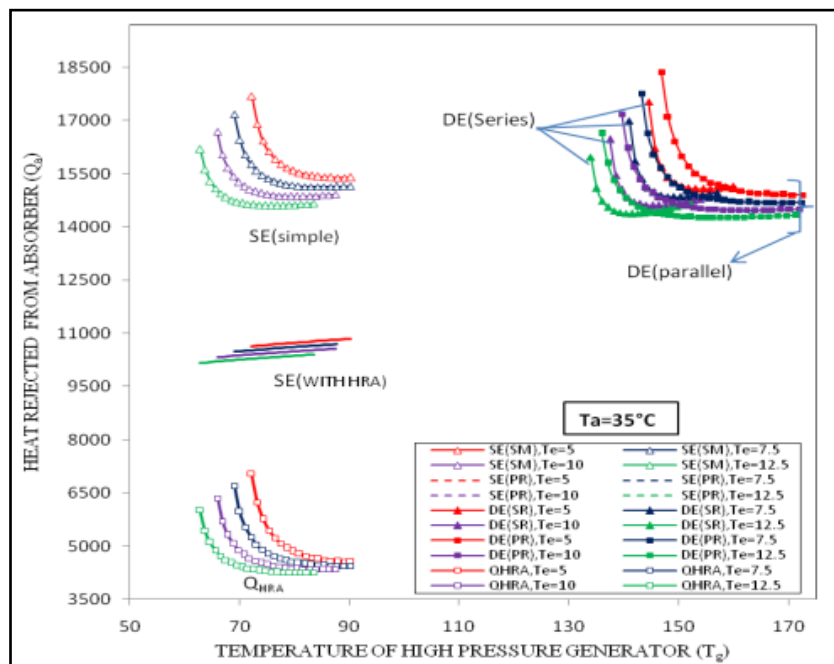

Fig. 9 Variation in the absorber load with the generator temperature for the single effect and the double effect cycles.

V.   CONCLUSIONS

a. In the single effect cycle using HRA, with refrigerant parallel flow, COP increases with increase in the values of refrigeration distribution ratio (RDR). The optimum value obtained is, RDR =0.3.

b. In the double effect parallel and series flow cycles, COP increases more drastically with increase in the high pressure generator temperature (T_g) as compared to the single effect cycle.

c. COP of the double effect parallel flow cycle, increases on increasing the solution distribution ratio (SDR). The optimum value of SDR obtained is 0.45.

d. Use of HRA with refrigerant parallel flow, in the single effect cycle results in around 24% increases of COP.

e. Similarly, increase in COP of the double effect parallel flow cycle from that of the series-flow-cycle is around 4 to 7%.

f. And, increase in COP of the double effect parallel flow cycle from that of the single effect simple cycle is around 75 to 77%.

g. Around 30% decrease in the absorber cooling load is observed with the use of HRA in the single effect cycle.

REFERENCES

[1]   Asdrubali F. and Grignaffini S., Experimental evaluation of the performances of a H_2O-LiBr absorbtion refrigerator under different service conditions, International Journal of Refrigeration, Vol. 28: 489-497, 2005.

[2]   Siddiqui, M.A., Optimum Generator Temperature in Four Absorption Cycle Using Different Sources of Energy, Energy Conversion and Management, No.24:251-266, 1993.

[3]   Gommed, K. and Grossman, G., Performance analysis of staged absorption heat pumps: water Lithium bromide systems, ASHRAE Transactions, 90-30-6:1590-1598, 1990.

[4]   Lee, S.F. and Sherif, S.A., Second Law Analysis of Multi Effect Lithium Bromide/Water Absorption Chillers, ASHRAE Transaction, AT-01-9-5:664-673, 2001.

[5]   Khaliq, A. and Kumar, R., Exergy Analysis of Double Effect Vapour Absorption Refrigeration System, International Journal of Energy Research, DOI:10.1002/er.1356, 2007.

[6]   Arun, M.B., Maiya, M.P. and Murthy, S.S., Performance Comparison of Double Effect Parallel Flow and Series Flow Water-Lithium Bromide Absorption Systems, Applied Thermal Engineering, 21:1273-1279, 2001.

[7]   Oh, M.D., Kim S.C. and Kim, Y.L., Cycle Analysis of an Air-Cooled Libr/H_2O Absorption Pump of Parallel-Flow Type, International Journal of Refrigeration, 17(8), 555-565, 1994.

[8]   Xu, G.P and Dai, Y.Q., Theoretical Analysis and Optimization of a Double-Effect Parallel Flow Type Absorption Chiller, Applied Thermal Engineering , 17(2):157-170, 1997.

[9]   Wang, L., Chen, G.M., Wang, Q. and Zhong, M., Thermodynamic performance analysis of a gas fired air cooled adiabatic absorption refrigeration systems, Applied Thermal Engineering, 27: 1642-1652, 2007.

[10]   Kaushik, S.C. and Kumar, R., Thermodynamic Feasibility of an Absorber Heat Recovery Cycle for Solar Air Conditioning, Heat Recovery Systems, **5**, 117, 1985.

[11]   Kandlikar, S.G., A New Absorber Heat Recovery Cycle to Improve COP of Aqua-Ammonia Absorption Refrigeration System, ASHRAE TRANSACTION, 88, 141-158, 1982.

[12]   Saghiruddin and Siddiqui, M..A., Economic Analysis and Performance Study of Three Ammonia-Absorption Cycles Using Heat Recovery Absorber, Energy Conversion and Management, No.37, pp 421-432, 1996.

[13]   Saghiruddin and Siddiqui, M.A. , Effect of Using a Heat Recovery Absorber on the Performance and Operating Cost of the Solar Ammonia Absorption Cycles, Journal of Solar Engineering , 119, 19-23, 1997.

[14]   Siddiqui, M. Altamush, Ph.D. Thesis AMU Aligarh, 1992.

[15]   Kaita, Y., Thermodynamic Properties of Lithium Bromide-Water Solutions at High Temperatures, International Journal of Refrigeration, 24:374-90, 2001.